

Colour image segmentation algorithm in vectoral approach for automated optical inspection in electronics

W. TARNAWSKI*

Systems and Computer Networks, Faculty of Electronics, Technical University of Wrocław,
27 Wybrzeże Wyspiańskiego Str., 50-370 Wrocław, Poland

This paper presents the robust colour image segmentation algorithm which can be used extensively in automated optical inspection system on the printed circuits boards (PCB) assembly line. The robustness of the presented algorithm is increased by low computational effort what dedicates this approach to on-line vision systems explored in high-speed production lines. The second advantage of the proposed algorithm is the non-parametric solution which is invariant to changes of light and colour of the inspected components. This condition should be fulfilled with the vectoral imaging approach where the most important task is the segmentation process which divides image space into disjoint regions with similar colour or texture.

Keywords: image analysis, colour image segmentation, clustering, optical inspection.

1. Introduction

Over the past two years, vectoral imaging technology has emerged as a real solution to the requirement of inspecting populated printed circuits boards at the speeds compatible with today's high-speed production lines. This approach is relatively fast and is not adversely affected by changes in colour, background, size, and rotation. Vectoral imaging technology is a pattern location search technology based on geometric feature extraction rather than absolute colour pixel values. Patterns are not dependent on the pixel grid. A feature is a contour that represents boundary between dissimilar regions in the image. Industrial standards allow for changes in both size and shape of components which are acceptable in industry. Any vision system used for this application has to take into account as well as the changes in appearance due to vendor variations and different manufacturing processes. Another major advantage with vectoral approach is the elimination of background features that may cause false failures. With inspecting the same component on different printed circuit boards, the board layout changes dramatically due to circuitry and density. This can induce false failures when using classical correlation approach used in template matching. That is why the image segmentation is the first and very important process in automated optical inspection based on the vectoral imaging.

Segmentation is a process of dividing an image into different regions such that each region is homogeneous but the union of any two adjacent regions is not. Many of the existing colour image segmentation approaches [1,2] are based on the monochrome segmentation techniques where the sin-

gle components R , G , and B or their transformations (linear/non-linear) are explored independently of the others. The results obtained from these single components are often difficult for unambiguous interpretation. To overcome this shortcoming, the analysis of the multidimensional feature space is required. The analysis of this space is very often time-consuming particularly in case of computer vision problems where a large "mass of the data" is connected to the image. The approach proposed in this paper is based on one of the widely used techniques for feature space analysis called clustering. The points in the feature space correspond to feature vectors describing points (pixels) in the image space. Colour images can be characterized by three-dimensional histograms, and thus, we have three-dimensional feature space in which clusters or modes correspond to pixels with similar colours called image regions.

One of the drawbacks of the feature space clustering is that the cluster analysis does not utilise any spatial information from the image space that considers the spatial relation among pixels. The second and the most serious problem is difficult determination of the number of clusters (image regions) in the unsupervised clustering scheme which is known as cluster validity. The next, crucial problem for the colour image segmentation is the selection of the appropriate colour space (feature space). RGB colour space is not appropriate for colour space clustering because of the high correlation of among R , G , and B , therefore an object with a uniform colour but different intensities could be segmented into different objects. In other words, a colour image with shadows or some shading cannot be segmented properly in RGB colour space. The proposed algorithm is based on the modified HSI colour space. The modification of HSI colour space has been already presented in Ref. 3

* e-mail: tarnawski@zssk.pwr.wroc.pl

where accurate analysis of this colour space is included. The advantage of the *HSI* colour space for the task of image segmentation is invariance to changes of the light what next implicates that data in this feature space will be coherent and well separated. The last problem is connected with the fact that real images always include some “lack of precision” or fuzziness. That is why it seems naturally to map colour space into the fuzzy domain that takes into consideration this characteristic.

In this paper, the colour segmentation algorithm is presented that performs colour image clustering based on the novel interpolated multi-resolution density function approximation in the modified and “fuzzified” feature space. The proposed method is not burden with the problems mentioned above. Block diagram of the proposed method is presented in Fig. 1.

The paper is organized as follows. In the first section, the concept of spatial feature based on the fuzzy homogeneity vector is presented [4]. The next section deals with mapping of the colour space feature into the fuzzy domain. The degree of fuzziness of the image is next measured by the inverse entropy. The following section describes the in-

multi-resolution idea is also introduced. On the basis of this measure, the input parameters are changed for the presented approximation. The last section demonstrates the segmentation results and effectiveness of the proposed technique in the task of the automated optical inspection system on the printed circuits boards (PCB) assembly line.

2. Fuzzy homogeneity vector as the spatial feature

The proposed method takes into account not only information from the colour space but also considers the spatial relation among the pixels described by the angle-related quantity called a homogeneity vector [4]. With every pixel $I(p)$ from the image I , the neighbouring pixels of the distance d angularly related to the pixel p are associated.

Let our colour space C will be modified *HSI** colour space described in Ref. 3 and the values $c(i,j)$ and $c(k,l)$ are the colours of two pixels located at (i,j) and (k,l) in the image I , where $C \in \mathbb{R}^3$ and $c \in C$. The degree of homogeneity between these two pixels is expressed by $\delta_Z(\|c(i,j) - c(k,l)\|)$ and $\delta_Z(x)$ is defined as follows

$$\delta_Z(x) = Z(x, a, b, c) = \begin{cases} 1 & 0 \leq x \leq r \\ 1 - 2[(x - a)/(c - a)]^2 & r \leq x \leq 1 \\ 2[(x - c)/(c - a)]^2 & s \leq x \leq t \\ 0 & t \leq x \leq \max\|c(i,j) - c(k,l)\| \end{cases} \quad (1)$$

terpolated multi-resolution density function approximation. In the same section, the cluster validity measure based on

where $x = \|c(i,j) - c(k,l)\|$, the symbol $\| \|$ means Euclidean’s metric, and $r, s,$ and t are the parameters.

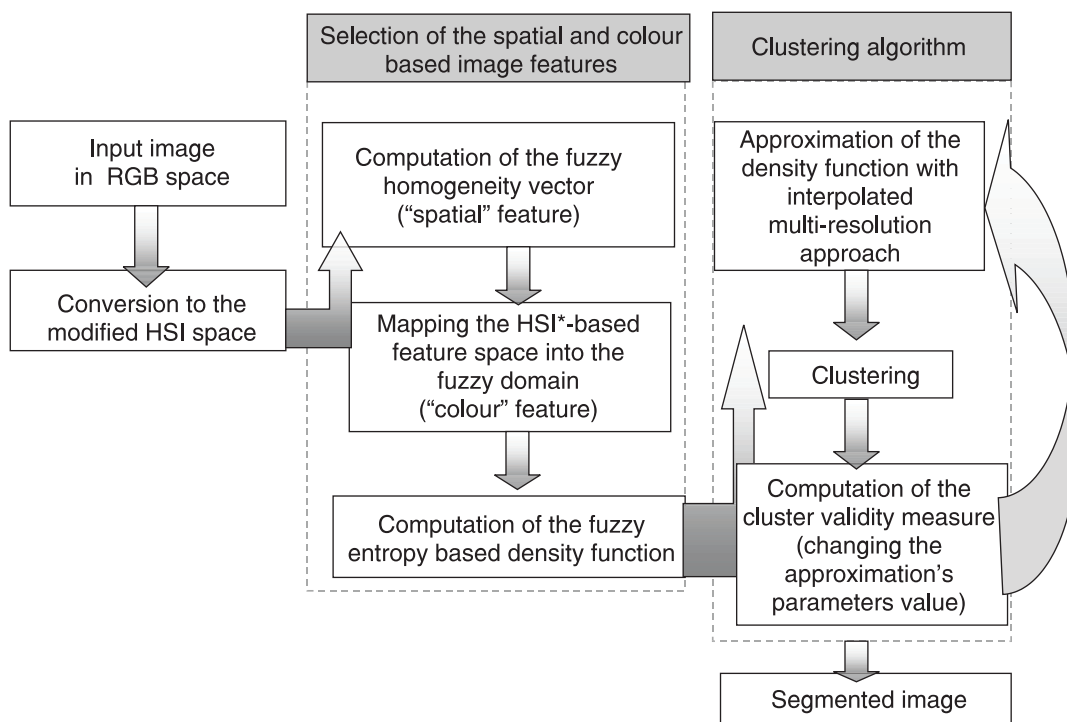


Fig. 1. The block diagram of the proposed color segmentation algorithm.

The property of homogeneity could be characterized by the vectors $h(c,d)$ which sum the degree of homogeneity occurring between the pixels with colour $c \in C$ and its neighbours with different angular θ and the neighbouring distance d defined as follows

$$h(c^*,d) = \left\{ \frac{1}{8} \sum_{\theta} \delta_Z \left(\|c^*(i,j) - c(k,l)\| \right), [c(i,j), c(k,l) \in C], [(i,j), (k,l) \in I] \right\}, \quad (2)$$

$$\left\{ \begin{array}{l} |(i,j) - (k,l)| = d \text{ along } \theta \end{array} \right.$$

where $\theta = 0^\circ, 45^\circ, 90^\circ, 135^\circ, 180^\circ, 225^\circ, 270^\circ, 315^\circ, d = 1$ and c^* denotes the colour of the reference pixel. Due to symmetric nature, these eight fuzzy homogeneity vectors could be reduced to four vectors. We could average the resulting four angular fuzzy homogeneity vectors to obtain the homogeneity vector $h(c^*,d)$ which will diminish the effect of rotation

$$h(c^*,d) = \frac{1}{4} [h(c,0^\circ,d) + h(c,45^\circ,d) + h(c,90^\circ,d) + h(c,135^\circ,d)] \quad (3)$$

3. Fuzzy entropy based spatial and colour feature's density distribution construction

Let $F = (f_1, f_2, \dots, f_L)$, where $F \in \mathbb{R}^3$ and $L = \{1, 2, 3, \dots, 2^{24}\}$ be a set of fuzzy membership values which are obtained by mapping the colour space C into the fuzzy domain $C \rightarrow F$ using the membership standard S function δ_S [5] and is defined as

$$f_a = \delta_S(c), \quad (4)$$

where $a \in L$.

The real images always include some "lack of precision" or fuzziness, which in colour images is represented as "light/dark colour" or rather "more/less saturated colour". That is why it seems naturally to map the saturation component c_{Sat} into the fuzzy domain as the following

$$f_a = \delta_S(c_{Sat}). \quad (5)$$

When the pixel membership value f_i equals 1.0, it means that it has complete (pure) colour and when $f_i = 0$ the colour information is not included. For $f_i = 0.5$ we receive the maximum fuzziness. The degree of fuzziness was usually measured by the entropy E under the fuzzy set F and in the previous work it was used for image thresholding [6]

$$E(F) = \frac{1}{MN \ln 2} \sum_{x=1}^M \sum_{y=1}^N S[\delta_S(c_{Sat}(x,y))], \quad (6)$$

where M and N are the numbers of rows and columns of the image I , respectively, and $S(\alpha)$ is the Shannon's entropy function defined as

$$S(\alpha) = -\ln \alpha - (1 - \alpha) \ln(1 - \alpha). \quad (7)$$

When $\alpha = 0$ or $\alpha = 1.0$ we receive minimum and when $\alpha = 0.5$ the maximum entropy value. In our case it should be interpreted that the pixels with minimum entropy form

pure colour or colourless (monochromatic) image regions and with maximal entropy the regions with maximal fuzziness. The clustering algorithm requires feature (colour) space in which modes (peaks) could be interpreted as colour or monochromatic image regions. These modes will become cluster prototypes, i.e., the points with minimal fuzziness. Therefore for this reason the Shannon entropy function $S(\alpha)$ should be reformulated into $S^*(\alpha)$ according to the formula

$$S^*(\alpha) = \begin{cases} 0 & \alpha = 0 \vee \alpha = 1 \\ S(0.5) - S(\alpha) & \text{otherwise} \end{cases} \quad (8)$$

Finally, the fuzzy entropy-based density distribution on the feature space that combines spatial information as the fuzzy homogeneity vector and the fuzzy colour property can be reformulated from Eq. (6) to the following

$$E(F) = \frac{1}{MN \ln 2} \sum_{x=1}^M \sum_{y=1}^N S^* \{ \delta_S(c_{Sat}(x,y)) \} \cdot h[c(x,y),d], \quad (9)$$

where the following conditions are fulfilled

$$\begin{cases} S^* \{ \delta_S(c_{Sat}(x,y)) \} \in < 0,1 > \\ h[c(x,y),d] \in < 0,1 > \end{cases} \quad (10)$$

4. Interpolated multi-resolution approach for density function approximation

The pixel's attributes of a colour image can be represented as a 3D vector in the feature space F described in the previous section. The only one constraint is that this space should be isotropic, i.e., the distance between any two points is independent on their location.

Let $E(F)$ be the histogram-type function, which represents the sum of the entropies for all pixels from the image located in the fuzzy domain F , according to Eq. (5). The distribution $E(F)$ of the image can be spread, and can also be condensed. The only constraint is that the feature space volume is limited. The feature space is of the size of $256 \times 256 \times 256$. The proposed method assumes that analysed feature space is quantised into cuboids. The size of a single cuboid is always $2^{p_x} \times 2^{p_y} \times 2^{p_z}$ where p_x, p_y , and

p_z denote the sizes on every dimension. This assumption makes possible further fast computation by using bit shift operations. The every single cuboid is divided into four cuboids, every of size: $2^{(p_x-1)} \times 2^{(p_y-1)} \times 2^{(p_z-1)}$. The idea of a cuboid's definition in feature space is presented in Fig. 2.

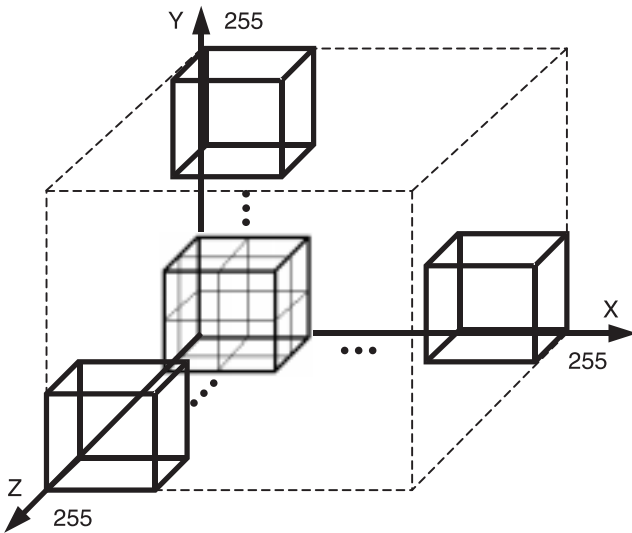


Fig. 2. The idea of cuboid's definition in the feature space.

The set of cuboids about the same size defines a single grid. The number and the size of the grids are the method's parameters which decide about the final approximation. The algorithm counts, through out the grids, the values $E_i(x',y',z')$ included in the cuboid $V_{x',y',z'}^i$ indexed in i -th grid by (x',y',z') according to the following

$$E_i(x',y',z') = \sum_{F_l \in V_{x',y',z'}^i} E(F_l). \quad (11)$$

The value of the density function $g_i(x,y,z)$ is therefore defined as the following

$$g_i(x',y',z) = E_i(x',y',z') / V_{x',y',z'}^i, \quad (12)$$

where $V_{x',y',z'}^i$ is the volume of the cuboid. The values of the density function $g_{i-1}(x',y',z')$ received in the $(i-1)$ -th grid differ from $g_i(x',y',z')$ in the "size of working" and the precision. The more dense grids there are, the more they are "able to detect" local peaks (modes) in opposite to fewer dense grids, in which the global modes are "better seen" what effects on densities like low-pass filtering.

The mean interpolated density function approximation for i -th grid at any point (x,y,z) is defined as following

$$\bar{g}_{interpol}^i(c) = \left(\sum_{k=1}^M g_i(p_k) V_k \right) / V_{x',y',z'}^i, \quad (13)$$

where p_k are the centroids of the nearest neighbours of the point reference point located at coordinates (x,y,z) , V_k are

the volumes of subcuboids (in Fig. 3 depicted as V_1, V_2, V_3, V_4) and M is the number of the nearest neighbours. The geometric scheme of this definition is presented in Fig.3 (for simplicity depicted in 2D)

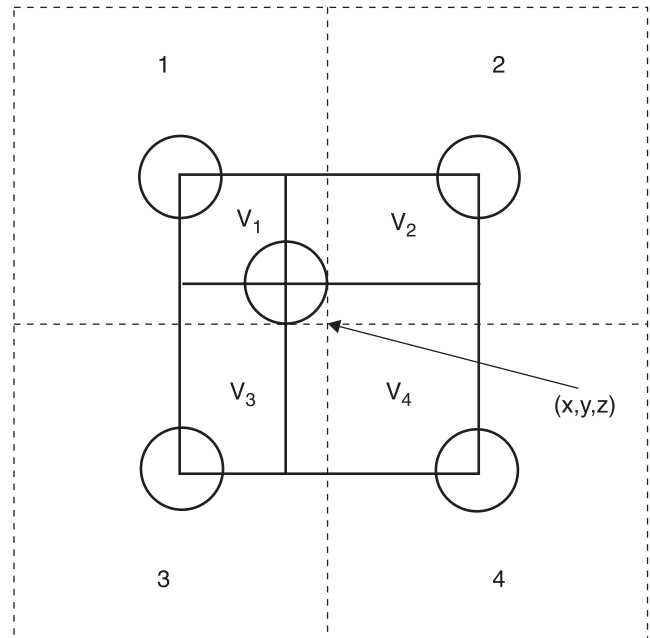


Fig. 3. The geometric scheme of the interpolated density function approximation at point located at coordinates (for simplicity depicted in 2D).

The multi-resolution conception is based on the fact that grids of the different sizes take into consideration the contribution of the density distribution at the different resolutions (multi-scale approach). The final definition of the interpolated multi-resolution density function $g(x,y,z)$ is therefore weighted superposition of the density function at the different resolutions described by the formula

$$g(x,y,z) = \sum_{i=1}^K w_i \cdot \bar{g}_{interpol}^i(x,y,z), \quad (14)$$

where w_i are the values (weights) of the Gaussian distribution $N(p_i, s)$ located at the centroids p_i of the cuboids in the i -th grid and K is the number of grids (s means the standard deviation).

5. Clustering algorithm and cluster validity measure

The clustering is performed by locating the peaks of the approximated three-dimensional entropy distribution $g(x',y',z')$ in the most dense grid where cells are indexed by triplet (x',y',z') . This is done by a peak-climbing (valley-seeking) algorithm developed by Koontz, Narendra, and Fukunaga [7]. The procedure is illustrated in

0	4 ← 2	0	0	0
17 →	65 ↓	0	0	21 ↓
4 →	31 ↑	20 ←	0	70 ←
0	0	0	29 →	93 ←
0	0	0	15 →	40 ↑

Fig. 4. Illustration of the peak climbing approach in two-dimensional space.

two-dimensional space in Fig. 4, where the number in each cell represents hypothetical values $g(x',y',z')$ in points of which are the centroids of the cells.

The maximal bins become cluster prototypes and the bins related to this prototype belong to this cluster. It is clear that input parameters: the cell's size in the most dense grid and the number of the grids play a major role in the success of the algorithm. A very small cell size would produce a flat distribution with no significant peaks, while too large may combine several peaks into a single mode, giving erroneous results in segmented image in form of the merged regions.

As it can be seen in Figs. 5(a) and 5(b), the number of the grids with the same size of the smallest cuboid affects the values of $g(x',y',z')$ in the following way: if close to the any mode is located another not so much smaller mode the values of $g(x',y',z')$ increase rapidly. Therefore it means that this cluster prototype "attracts" the nearest smaller modes that cause increasing $g(x',y',z')$.

In practice (segmentation's result), it results in merging significant and similar colour image region which is not desired. Let $\Delta g_{(i, i+k)}(x',y',z')$ be the difference between the

density values in i -th grid and $(i+k)$ -th grid ($k \in \{1,2,3,4\}$) defined by the Camber's measure

$$\Delta g_{(i,i+k)}(x',y',z') = 1 - \frac{|g_i(x',y',z') - g_{(i+k)}(x',y',z')|}{g_i(x',y',z') + g_{(i+k)}(x',y',z')} \quad (15)$$

where

$$\Delta g_{(i, i+k)}(x',y',z') \in \langle 0.1 \rangle$$

Based on this difference, the cluster validity measure Φ is defined in order to express the cluster separability which is identified as the cluster validity measure

$$\Phi(P_1, \dots, P_L) = \sum_{m=1}^L \sum_{n \neq m} |\Delta g_{(m,m+4)}(P_m) - \Delta g_{(n,n+4)}(P_n)| \|d(P_m, P_n)\| \quad (16)$$

where L is the found cluster number, the symbol $\| \|$ means a norm, and d is the Euclidean distance. The optimal number of L clusters and the location of the cluster prototypes are met when this measure is maximized, i.e.,

$$\Phi = \max \{ \Phi(P_1, \dots, P_L) \}. \quad (17)$$

In the task of the automated optical inspection system, the procedure of adjusting the input parameters for the proposed approximation on the basis of the proposed measure Φ is computationally expensive. However, this procedure can be executed only one time during the "learning" process which is realized by operator at the beginning. For every frame (image), the adjusted parameters are saved in a special memory and during testing they are treated as *a priori* information about the analysed image.

6. Results and conclusions

The proposed algorithm has been tested in the task of the automated optical inspection system on the printed circuits boards assembly line. The frames (images) were acquired by camera SONY DFW-V500 with resolution 640x480

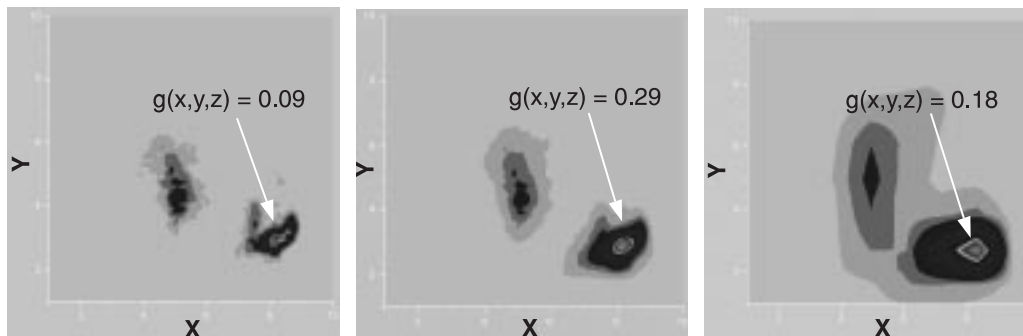


Fig. 5. The graph of the interpolated multi-resolution density for the different number of grids and minimal cuboid size (for $z = 85$) a) 1 grid, minimal cuboid's size: $2^3 \times 2^3 \times 2^3$ b) 4 grids, minimal cuboid's size: $2^3 \times 2^3 \times 2^3$ c) 1 grid, minimal cuboid's size: $2^5 \times 2^5 \times 2^5$.

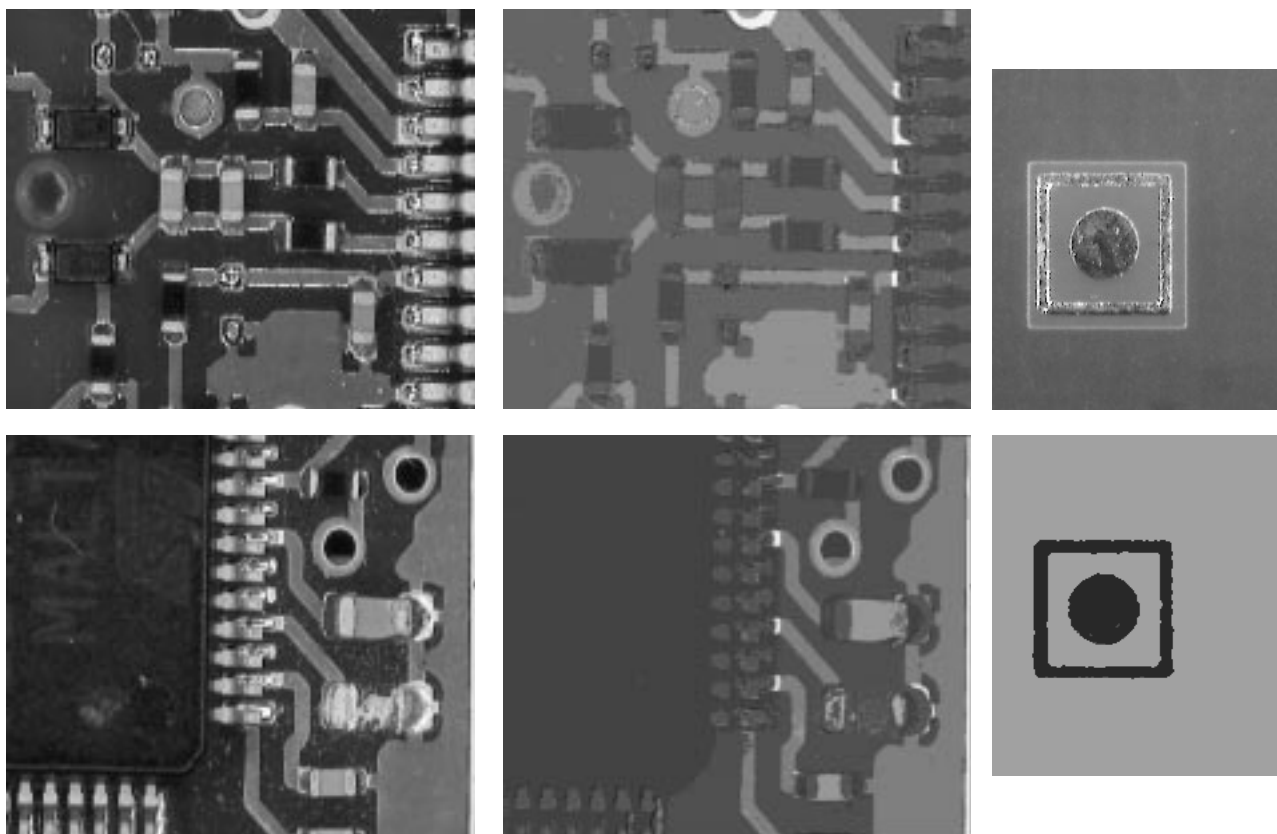


Fig. 6 Segmentation results obtained for images analyzed in the tasks of the automated optical inspection on the printed circuits boards (PCB) assembly line.

pixels. The upper limit of the time processing for the segmentation process per one frame was 0.07 s. The algorithm was implemented on the processor AMD ATHLON 1.5 GHz. The tests revealed that the proposed algorithm was able to segment images in the time about 0.05 s. A few result images from this process are presented in Fig. 6.

The proposed algorithm minimizes the following limitations met very often in the colour image segmentation:

- need of specifications of some *a priori* knowledge about the analysed image or other parameters which control the segmentation process,
- slowness due to extensive computations required,
- invariance to changes of the light.

Segmented image makes possible easy and simple contour's definition that represents boundary between dissimilar regions in the image what is the basis for the vectoral imaging approach.

References

1. N.R. Pal and S.K. Pal, "A review on image segmentation techniques", *Pattern Recognition* **29**, 1277–1294 (1993).
2. K.S. Fu and J.K. Mui, "A survey on image segmentation", *Pattern Recognition* **13**, 3–16 (1981).
3. W. Tarnawski, "Fast and efficient colour image segmentation based on clustering modified *HSI* colour space", *Proc. 4th Sci. Symp. on Images Processing Techniques*, Warsaw University of Technology, Serock, 244–257 (2002). (in Polish)
4. Ch.D. Cheng, X.H. Jiang, and J. Wang, "Colour image segmentation based on homogram thresholding and region merging", *Pattern Recognition* **35**, 373–393 (2002).
5. S.K. Pal and D.K. Dutta Majumder, *Fuzzy Mathematical Approach to Pattern Recognition*, Wiley & Sons, New York, 1986.
6. W. Tarnawski and A. Merta, "Colour image segmentation based on fuzzy rules derived from entropy measurement", *Machine Graphics & Vision* **9**, 487–495 (2000).
7. K. Fukunaga, *Introduction to Statistical Pattern Recognition*, Academic Press, New York, 1990.